sciendo

DOI: 10.2478/awutp-2023-0011

ANNALS OF WEST UNIVERSITY OF TIMISOARA PHYSICS
Vol. LXV, 2023

STRUCTURAL AND OPTOELECTRONIC PROPERTIES OF CUBIC PEROVSKITE TYPE $XAlO_3$ (X = Gd AND Dy) THEORETICAL INVESTIGATION

Bouhenna Abdelkder [1], Benyahia Karima[1], Beloufa Nabil[2,3], Boualem Kada[1] and Bekheira Samir[4]

[1]Materials Science and Applications Laboratory (LSMA), Faculty of Sciences and Technology, University of AinTemouchent, BelhadjBouchaib.BP 284, Ain-Temouchent, 46000, Algeria
[2]Hydrometeorological Institut for Formation and Research IHFR, Oran, Algeria.
[3]Laboratory of Micro and Nanophysics (LaMiN), National Polytechnic School Oran, ENPO-MA, BP 1523, El M'Naouer, 31000, Oran, Algeria.
[4]Laboratory of Materials (LabMat), National Polytechnic School Oran, ENPO-MA, BP 1523, El M'Naouer, 31000, Oran, Algeria.
**Corresponding author: abdelkader.bouhenna@univ-temouchent.edu.dz*
karima.benyahia@univ-temouchent.edu.dz

Article Info

Received:23.08.2023
Accepted: 02.11.2023

Keywords:
Perovskite, $GdAlO_3$, $DyAlO_3$, FP-LAPW, GGA-PBE, mBJ

Abstract

In this paper, we have performed a theoretical study using the linear augmented and linearized plane wave method (FP-LAPW) implemented in the Wien2k computational code based on density functional theory (DFT) to determine the structural, electronic and optical properties of $GdAlO_3$ and $DyAlO_3$ perovskites. The exchange and correlation potential are treated by the generalized gradient approximation of Perdew-Burke-Ernzerhof (GGA-PBE) and modified Becke-Johnson potential (mBJ). The structural properties such as lattice parameter, modulus of compressibility and its derivative are in good agreement with other theoretical results.

The electronic properties, such as band structure and density of state revealed an indirect energy gap in the L - xG direction for $GdAlO_3$, with gap values of 2.879 eV (GGA-PBE), 5.006 eV (mBJ) in spin-up and 2.286 eV (mBJ), 2.736 eV (mBJ) in spin-dn.for $DyAlO_3$ perovskite, due to the over lap of the valence and conduction bands at Fermi level, which behaves like a metal oxide.

We have also calculated the optical properties of these two compounds, such as dielectric function, refractive index, absorption coefficient and optical conductivity. They indicate that $GdAlO_3$ and $DyAlO_3$ perovskites could be useful for applications in UV photo catalysis.

1. Introduction

The structure of perovskite is a general form ABC_3, with cation A in the corner, B in the middle and anion C on the faces of the cubic cell [1]. The A cation is coordinated with twelve

atoms and the B cation is assigned with six atoms, so the structure resembles a lattice of BC_6 octahedra divided at the corner, where all B-C-B angles are 180º[2, 3], the majority of these compounds are found in oxides ($GdAlO_3$, $DyAlO_3$), fluorides ($CsPbF_3$, $RbZnF_3$), heavier halides and hydrides, sulfides [4,5] . Cubic perovskites are recognized as ideal perovskites with the Pm3m (#221) space group [6]. Materials in this class have great potential for a variety of device applications due to their simple crystal structure and unique dielectric and ferroelectric properties [7, 8]. They have come into widespread use as a buffer or substrate material for oxide thin films and the heteroepitaxial growth of high-temperature superconductors [9]. The successful fabrication of large GaAs MOSFETS on Si substrates using cubic perovskite as a buffer layer has increased interest in these compounds. [10] Due to the growing interest in these compounds, and their extensive use in existing technology and potential applications in futuristic high-tech devices, the study of the structural, electronic and optical properties of these perovskites is being used extensively [11]. The intrinsic properties of perovskite materials can change through modifications to their elements, offering a multitude of physical properties depending on the chemical and electronic nature of atoms A and B [12, 13], metal-insulator transition piezoelectricity/ferroelectricity [14, 15].

ABO_3 perovskite-type oxide materials have attracted growing interest for many years, thanks to the ease with which the nature of the A and B cations present in the structure can be changed (as required). Modifications to these elements lead to a change in the intrinsic properties of the material, producing new physical properties depending on the chemical and electronic nature of the A and B atoms [16]. According to scientific research, at high temperatures the space group to which cubic perovskite belongs is Pm-3m, the so-called prototype variety, corresponding to the para-electric structure [17]. On the other hand, as the temperature decreases, this compound can undergo various polar and non-polar phase transitions [18]. The ABO_3 form of perovskite is cubic in nature according to the origin of the lattice and the corresponding Wyckoff positions, but the researchers found that this cubic structure is not adopted by all ABO_3 compounds, as other crystalline structures ($LiNbO_3$, $YMnO_3$ or $BaThO_3$) can also be found, such as the hexagonal or orthorhombic structure [19]. The structural representation of perovskite can be performed by placing the origin on one of the two cations A or B, which corresponds mainly to the representation of Miller and Love [20].

The best-known example of a tetragonal perovskite is probably the form of ferroelectric $BaTiO_3$ at room temperature, with a = 3.994 Å, c = 4.038 Å and Z= 1. In this case, the TiO_6

octahedra are slightly distorted (one Ti-O bond at 1.86 Å, four at 2.00 Å and a longer one at 2.17 Å) [21].

The rhombohedral perovskites are $LaAlO_3$, $PrA1O_3$, $LaNiO_3$ and $LaCoO_3$. This last perovskite has a rhombohedral structure at room temperature, but at elevated temperatures it undergoes two interesting phase transitions [22], transforming into another rhombohedral phase (R_3c to R_3). Also, the trivalent cobalt is ordered in such a way as to have alternating (111) planes with spin-high and spin-low Co (III) ions [23]. In this structure, the FeO_6 octahedra are distorted and inclined. Other materials adopting this orthorhombic-distorted structure are $NaUO_3$, $NaMgF_3$, $LaYbO_3$ and a large number of lanthanide compounds of the type $LnCrO_3$, $LnGaO_3$, $LnFeO_3$, $LnMnO_3$, $LnRhO_3$.

The perovskites have an important role in industrial technology. They are used in memories, capacitors [24], microwave devices [25], pressure gauges and ultrafast electronics [26]. They are superconducting at relatively high temperatures [27], and convert mechanical pressure or heat into electricity [28], accelerate chemical reactions (catalysts) [29] and suddenly change their electrical resistance when placed in a magnetic field (magnetoresistance) [30]. Perovskites with transition metal (TM) ions occupying the B-site show an enormous variety of intriguing electronic and magnetic properties [31]. This variety is not only linked to their chemical flexibility, but also to the greater degree related to the complex character that transition metal ions play in certain coordinations with oxygen or halides [32]. While magnetism and electronic correlations are usually linked to unfilled 3d electron layers, pronounced dielectric properties are linked to filled 3d electron layers [33]. non-polluting dyes [34], photovoltaic cells [35] or fuel cells [36]. Perovskites can be used almost universally, as their properties can be varied within very broad limits. For this reason, A. Reller and T. Williams have called them "Perovskites - chemical chameleons" [37].

The main objective of this work is the theoretical study of the structural and optoelectronic properties of $XAlO_3$ type perovskites where (X = Gd and Dy) in the cubic phase using the wien2k calculation code [38] where the exchange and correlation potential has been treated by the generalized gradient approximation of Perdew-Burke-Ernzerhof (GGA-PBE) [39] and the modified Becke-Johnson potential (mBJ) [40]. This manuscript is composed of three sections organized as follows: The first part is a general introduction to perovskite materials. The second section briefly describes the methods and details of calculation. In the third section, the results and discussion of the various structural and electronic properties of $GdAlO_3$ $DyAlO_3$ are presented, together with a comparison with some experimental data and

other theoretical results. At the end, a conclusion and perspectives are presented.

2. Computational method and details

We have used the FP-LAPW linearized augmented plane wave method implemented in the WIEN2k code [38]. Exchange and correlation effects were treated by the following two approximations: generalized gradient approximation developed by Perdew-Burke-Ernzerhof (GGA- PBE) [39] for the purpose of underestimating energy gaps, and modified Becke-Johnson potential (mBJ) [40]. To better predict electronic properties and provide the best energy gaps with a precision closer to the experimental.

The most important parameters that need to be refined to perfectly describe the systems studied are: the radii of the muffin-tin spheres (RMT), where we have chosen Dy: (2.52 u.a), Gd: (2.50 u.a), Al: (1.79 u.a) and O: (1.77 u.a) respectively and the number of k points in the first Brillouin zone. For integration, K=100 corresponding to 27 special points was used for the compound $DyAlO_3$ and K=200 equivalent to 10 special points for the compound $GdAlO_3$. The parameters G_{max}, l_{max} and $R_{mt}.k_{max}$ were taken to be equal to 12, 10 , 7 and 12, 5, 7 for the compounds $DyAlO_3$ and $GdAlO_3$ respectively. For the electronic configuration we have treated the states: Dy: [Xe] $4f^{10}$ $5s^2$, Gd: [Xe] $4f^7$ $5d^1$, Al: ($1s^2$ $2s^2$ $2p^6$ $3s^2$ $3p^1$) and O: ($1s^2$ $2s^2$ $2p^4$).

The cut-off energy that defines the separation between core and valence states is taken-10 Ry. The core states are treated within the framework of complete relativism, while the valence states are treated within the framework of scalar relativism. Since we have a semiconductor and non-magnetic material, spin-orbit coupling effects are neglected because of their very small effect on the calculation of the different properties. Muffin-Tin radii (RMT) was taken equal to 2.12, 1.90, 1.70 u.a for Sn, Y, and O atoms, respectively. The electronic configuration of Tin is [Kr] $4d^{10}$ $5s^2$ $5p^2$, Yttrium is [Kr] $4d^1$ $5s^2$ and that of Oxygen [He] $2s^2$ $2p^4$.

3. Results and discussions

3. 1. Structural properties

The compounds $GdAlO_3$ and $DyAlO_3$ are members of the perovskite oxide family, with the general form ABO_3 , where the A^{m+} ion is an alkali metal, alkaline earth metal or rare earth element, and B^{n+} is a transition metal cation. Both our compounds are cubic perovskites that crystallize in the Pm-3m (#221) space group. The coordinence of O^{2-} and B^{n+} ions are 6, while

the A^{m+} cation is placed in the cuboctahedral cavity in coordinence 12 (Figure 1).

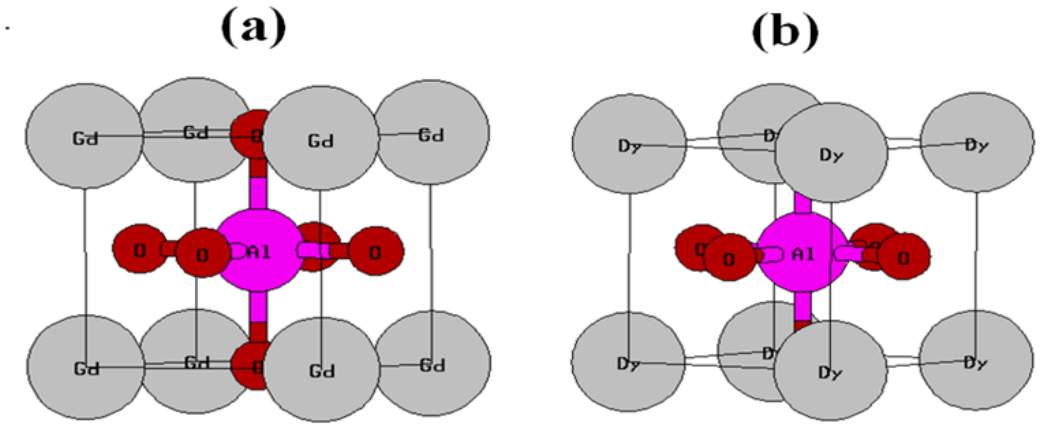


Figure 1. Cubic crystal structure of: (a) $GdAlO_3$ et (b) $DyAlO_3$ compounds by XCrysDen visualization program

The equilibrium structural parameters of the $GdAlO_3$ and $DyAlO_3$ compounds were determined by calculating the total energy for different lattice parameters and fitting the calculated values to the Birch-Murnaghan equation [41] given by the following formula:

$$E(V) = E_0 + \left[\frac{B_0 V}{B'(B'-1)}\right].\left[B'\left(1-\frac{V_0}{V}\right) + \left(\frac{V_0}{V}\right)^{B'} - 1\right] \quad (1)$$

Where V_0 is the static equilibrium volume of the primitive mesh, E_0 the total energy per primitive mesh of the equilibrium state, B is the modulus of compressibility and B' its derivative.

$$\acute{B}_0 = \frac{\partial B}{\partial P} \quad (2)$$

The volume V_0 and energy E_0 are given by the minimum of the E_{tot} curve (V) and the modulus of compressibility B_0 is determined by:

$$B_0 = V_0 \frac{\partial^2 E}{\partial V^2} \quad (3)$$

The variations of total energy as a function of volume for the two compounds are shown in Figure 2. The results obtained for the lattice parameter, the compressibility modulus and its derivative, are shown in Table 1. In order to compare our results with others, we have included in this table the theoretical results available in the literature for the two cubic perovskites $GdAlO_3$ and $DyAlO_3$.

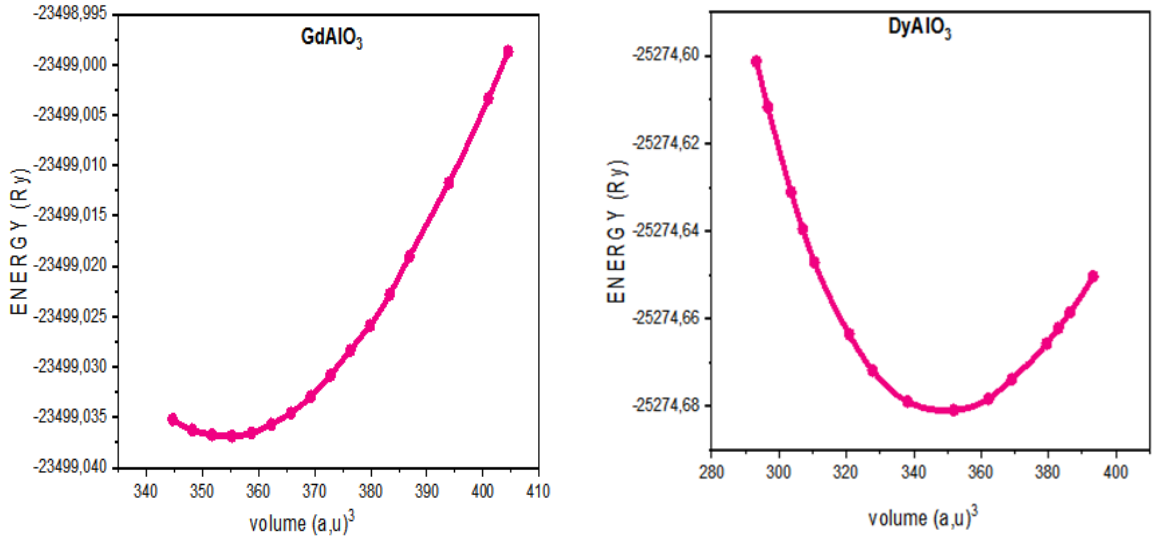


Figure. 2 Total energy versus volume for $DyAlO_3$ and $GdAlO_3$ perovskites

Table 1. The lattice parameter a_0, the compressibility modulus B_0 and its derivative B'_0 for the compounds $DyAlO_3$ and $GdAlO_3$ compared with other theoretical results.

Compound	a_0(Å)	V (u.a)^3	B(GPa)	B'	E$_0$ (Ry)
$GdAlO_3$	3.70* 3.7133 [a]	354.151* 350.88 [a]	202.341* 191.39 [a]	4.57* 4.4165 [a]	-23499.036* − 23498.46 [a]
$DyAlO_3$	3.73* 3.74[b]	348.874*	194.525* 207.52[b]	4.25*	-25274.680* −25 271.32[b]

*Present calculation, [a]Ref [42], [b]Ref [43]

We are not aware of any experimental work on the physical properties of $GdAlO_3$ and $DyAlO_3$ perovskites. In comparison, we note that our lattice parameters calculated from the GGA-PBE approximation are lower than those found theoretically by reference [42]. This underestimation is of the order of 1.02% for $GdAlO_3$ and 1.01% for $DyAlO_3$.

Note that our compressibility modulus values are considerably close to the theoretical data of Alsobhi [42] and Tariq Usman et. al. [43]; this agreement is explained by the use of the same calculation approach. We also note that the compressibility modulus values of the two compounds, $GdAlO_3$ and $DyAlO_3$, are quite similar. Overall, our results are in good agreement with the theoretical results [42, 43].

3. 2. Electronic properties

3. 2. 1. Band structure

The band structure describes the possible energies of an electron as a function of the wave vector. These bands are therefore represented in reciprocal space and, to simplify

calculations, only the directions of highest symmetry in the first Brillouin zone are treated. For oxide-perovskites of the $XAlO_3$ type (X = Gd and Dy), band structures are calculated in the first Brillouin zone along the directions of highest symmetry, with zero energy chosen to fix the Fermi level. The band structures of the $GdAlO_3$ and $DyAlO_3$ compounds were calculated using the FP-LAPW method, based on the GGA-PBE and mBJ approximations. Since the band structures obtained are very similar in appearance, with only a slight shift of a few bands, we present only the curves obtained in Figures 3 and 4.

Figure 3 shows that $GdAlO_3$ has an indirect gap in spin-up and spin-down: the valence band maximum is at the L point and the conduction band minimum is at the xG point. The gap values are approximately 2.879 eV (GGA-PBE), 5.006 eV(mBJ) in spin-up and 2.286 eV (mBJ)), 2.736 eV(mBJ) in spin-dn. whereas this compound behaves like an insulator in spin-up and like a semiconductor in spin-dn. We note that the $GdAlO_3$ compound exhibits a wide energy gap, which is a common feature of oxide-perovskites. The topology of our band structures is similar to that calculated by Alsobhi [42] and the energy gap values are in good agreement with those found theoretically.

In Figure 4, we show that the perovskite $DyAlO_3$ behaves like a metal oxide in spin up and spin down, due to the overlap of the valence band and conduction band at the Fermi level. Using the mBJ calculation, we show that from spin up, $DyAlO_3$ exhibits insulator behavior Eg=4.77eV and semiconductor behavior with an indirect band gap of Eg=0.698eV in spin-dn.

We note that there is a large discrepancy with the values obtained by the mBJ approximation. The latter is a modified version of the Becke and Johnson functional [40], and its application quickly proved highly effective in producing results for energy gaps very close to experiment. It should be noted that the modification brought about by the mBJ appears mainly in the conduction bands, the valence bands for all types of calculation being relatively the same.

All the energy gap results obtained from the two approximations are grouped together in Table 2 and compared with other theoretical calculations.

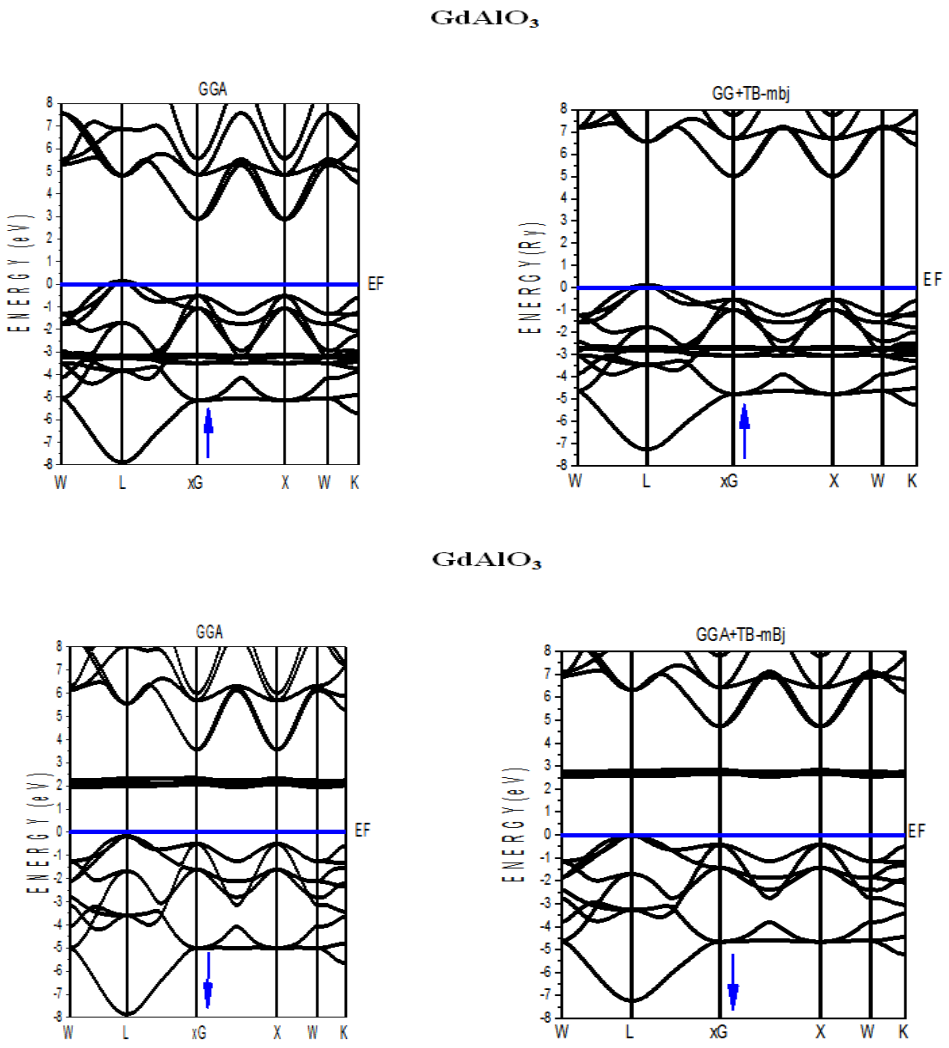
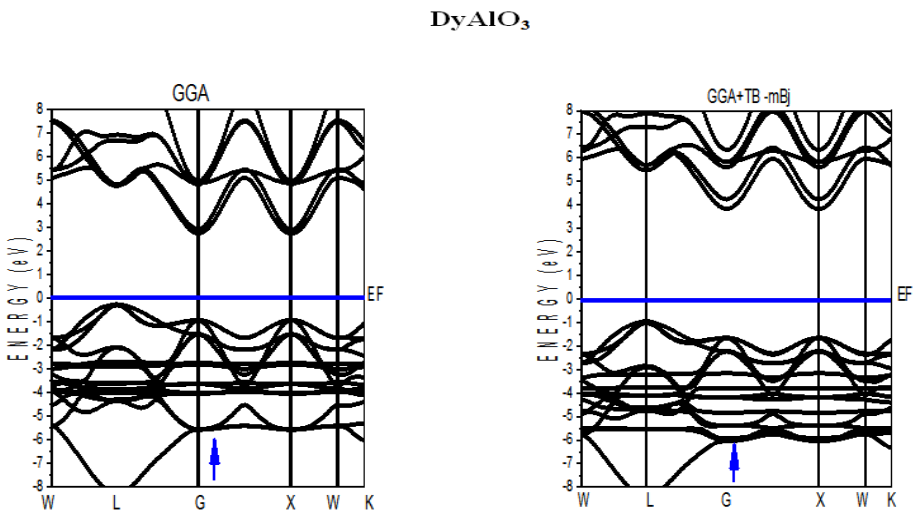


Figure 3. Band structure of $GdAlO_3$ using GGA-PBE (left panel) and mBj (right panel) approximation



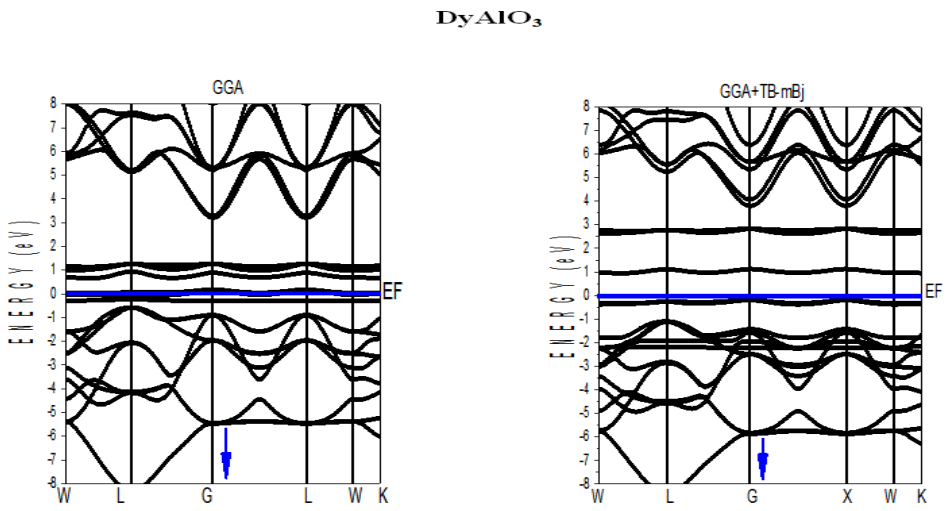


Figure 4. Band structure of $DyAlO_3$ using GGA-PBE (left panel) and mBJ (right panel) approximation

Table 2. The theoretical values of the different gaps for the compounds $GdAlO_3$ and $DyAlO_3$

Energy Band gap(eV)						
		This work		Theoretical calculations		Experiments
		GGA-PBE	mBJ	GGA-PBE	mBJ	
$GdAlO_3$	Up	2.879*	5.006*	2.851[a]	4.918 [a]	5.0 [c]
	Dn	2.286*	2.736*	1.882[a]	2.205 [a]	
$DyAlO_3$	Up	0*	4.77*	3[b]		5.15[d]
	Dn	0*	0.698*	0.2[b]		

* Present calculation, [a]Ref [42], [b]Ref [44], [c]Ref [50], [d]Ref [51]

3. 2. 2 Density of state (DOS)

The density of electronic states (DOS) is one of the most important electronic properties, providing information about the behavior and electronic character of a system. It also tells us about the nature of chemical bonds between atoms in a crystal or molecule. From the partial density of states (PDOS) curves, we can determine the predominant character of each region. Figures 5 and 6 illustrate the total and partial densities of states of the compounds $GdAlO_3$ and $DyAlO_3$ obtained using the mBJ approximation. The Fermi level is taken as the origin of the energies.

The total and partial densities of states of these two-spin perovskites, we can see that aluminum and oxygen atoms exhibit symmetry between the peaks of the two spins (Up and Dn) because they are not magnetic.

The Dy state gives rise to eight distinct regions separated by vacancies. The valence

band (BV) consists of six regions in the following energy ranges: from -5.90 eV to -5.36 eV, from -4.98 eV to -4.54 eV, from -4.54 eV to -3.64 eV, and from -3.64 eV to -3.04 eV in the spin-up part and from -2.45 eV to -1.50 eV and from -0.51 eV to -0.16 eV in the spin-dn part in band of conduction (BC) constituted two regions in an energetic interval only in the part spin-dn, from 0.76 eV to 1.11 eV and from 2.50 to 2.85 eV. The determination of the orbital characters for the energetic regions allows us to determine the value of the energy of band prohibited for our material.

Two distinct regions separate a given Gd atom by gaps due to the f-Gd state. In the valence band (BV) is a region in the following energy ranges: from -3.17 eV to -2.41 eV for spin-up, and from 2.46 eV to 2.85 eV in the conduction band (BC) for spin-dn.

In the case of $DyAlO_3$ and $GdAlO_3$, we note the difference between the peaks of the two spins, which confirms their ferromagnetic behaviour: the bottom of the valence band is dominated by the p-O, p-Al, s-Al states, and the bottom of the conduction band is mainly due to the f-Dy f- Gd states respectively.

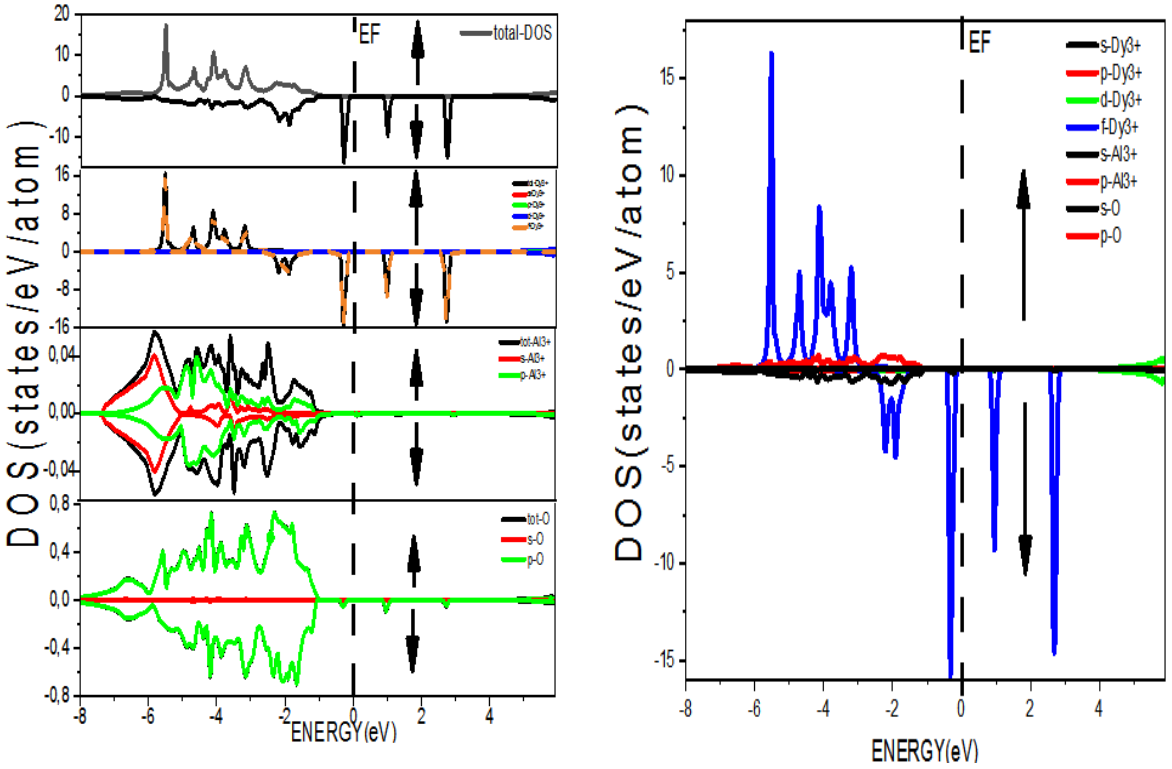


Figure 5. Partial and total density of state (PDOS and TDOS) of $DyAlO_3$

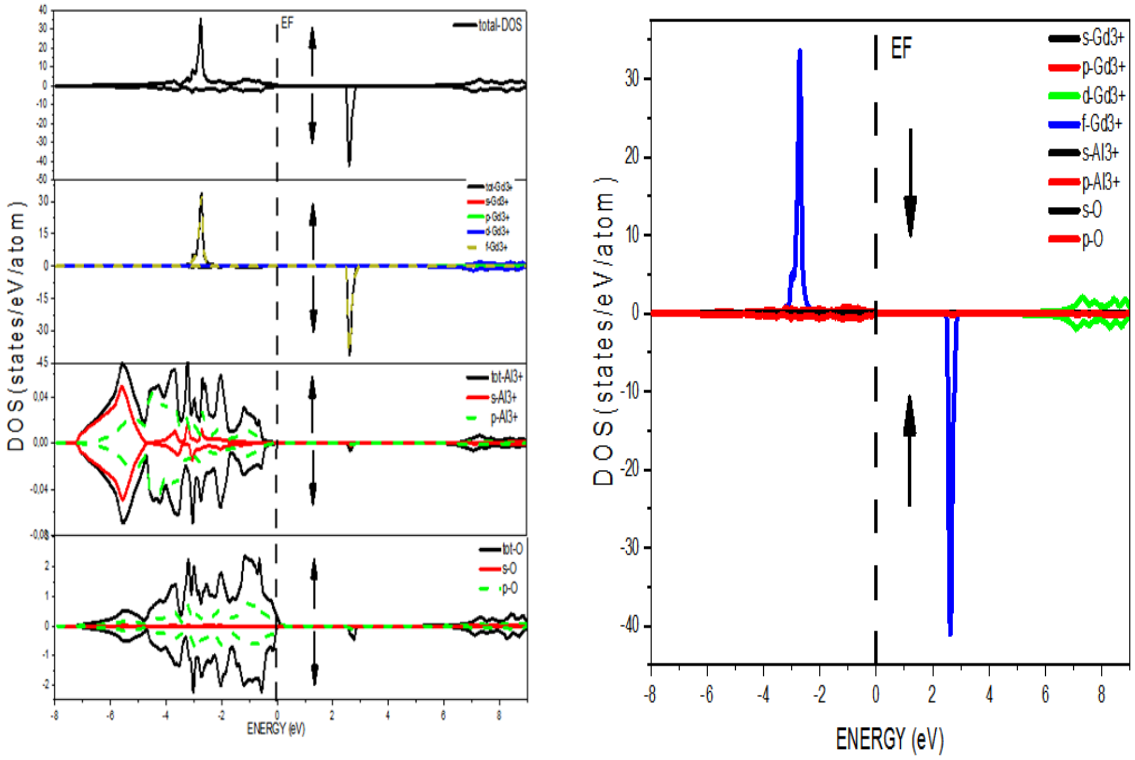


Figure 6. Partial and total density of state (PDOS and TDOS) of $GdAlO_3$

4. Optical Properties

4. 1. Dielectric function

The dielectric function ε(ω) is designed to describe the optical response of the medium at all photon energies and is defined by the following relationship [45]:

$$\varepsilon(\omega) = \varepsilon_1(\omega) + i\,\varepsilon_2(\omega) \tag{4}$$

The imaginary part $i\varepsilon_2(\omega)$ is directly related to the electronic band structure of both materials. This dielectric function $\varepsilon_2(\omega)$ is equal to:

$$\varepsilon_2(\omega) = \frac{8}{3\pi\omega^2}\sum_{n\dot{n}}\int |P_{n\dot{n}}(k)|^2 \frac{dS_k}{\nabla\omega_{n\dot{n}}(k)} \tag{5}$$

$P_{n\dot{n}}(k)$: are the elements of the dipole matrix between $|nk\rangle$ and $|\dot{n}k\rangle$

In this section, we present the optical properties as well as the dielectric function, refractive index, absorption coefficient and optical conductivity of cubic perovskites $GdAlO_3$ and $DyAlO_3$.

The electronic polarizability of a material can be understood from the real part of the

dielectric function $\varepsilon_1(\omega)$ (Figure 7.a) The mean value of the zero-frequency dielectric constant $\varepsilon_1(0)$ is 2.09 and 2.63 for $GdAlO_3$ and $DyAlO_3$ respectively in the cubic phase. From the zero-frequency limit, they begin to increase reaching maximum values of 3.07 to 7.25 eV for $GdAlO_3$ and 1.08 to 7.94 eV for $DyAlO_3$. The optical bandwidths obtained from the imaginary part of the dielectric function are 2.75 and 0.73 respectively for $GdAlO_3$ and $DyAlO_3$ perovskites, close to the deviations obtained in the band structures; the band gaps of this material are below 3.1 eV, which is not expected to work in the ultraviolet (UV) region [46, 47], and may not be suitable for high-frequency UV device applications.

The imaginary part of the dielectric function $\varepsilon_2(\omega)$ is shown in Figure 7.b. A wide range of absorption regions is observed with two main peaks. The first peak is obtained at 8.24 eV for $GdAlO_3$ and the second at 8.78 eV for $DyAlO_3$. The origin of these peaks lies in the inter-band transitions that can be related to the density of states of the compounds shown in Figure 6. The peaks are due to the transition of electrons from the 2p-O states to 3p-Al. As the material has a wide and direct bandwidth, it could be an effective candidate for optoelectronic applications in the visible range.

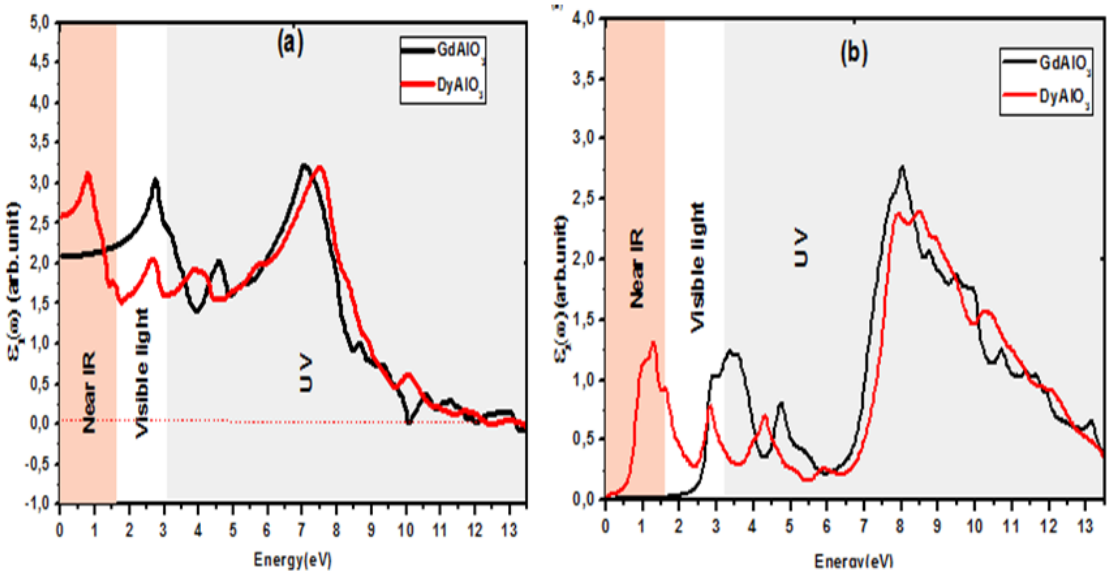


Figure 7. Real parts $\varepsilon_1(\omega)$ (a) and Imaginary parts $\varepsilon_2(\omega)$ (b) of the dielectric function of $GdAlO_3$ and $DyAlO_3$ using GGA + TB-mBJ

4. 2. Absorption coefficient, refraction index and reflectivity

The optical constants, such as refractive index $n(\omega)$, reflectivity $R(\omega)$, absorption coefficient $\alpha(\omega)$ and distinction coefficient $K(\omega)$, are calculated on the basis of the dielectric function, according to the following relationships [48, 49]. In complex form, the refractive index is expressed as:

$$N = n + iK \tag{6}$$

n (ω): the index of refraction.

k (ω): the extinction coefficient

$$n(\omega) = \frac{1}{\sqrt{2}}[(\varepsilon_1(\omega)^2 + \varepsilon_2(\omega)^2)^{1/2} + \varepsilon_1(\omega)\ ]^{1/2} \tag{7}$$

$$K(\omega) = \frac{1}{\sqrt{2}}\ [(\varepsilon_1{}^2(\omega) + \varepsilon_2{}^2(\omega)\ )^{1/2} - \varepsilon_1(\omega)\ ]^{1/2} \tag{8}$$

$$\alpha(\omega) = \frac{4\pi}{\lambda} k(\omega) \tag{9}$$

$$R(\omega) = \left|\frac{\sqrt{\varepsilon(\omega)}-1}{\sqrt{\varepsilon(\omega)}+1}\right|^2 = \frac{(n-1)^2+k^2}{(n+1)^2+k^2} \tag{10}$$

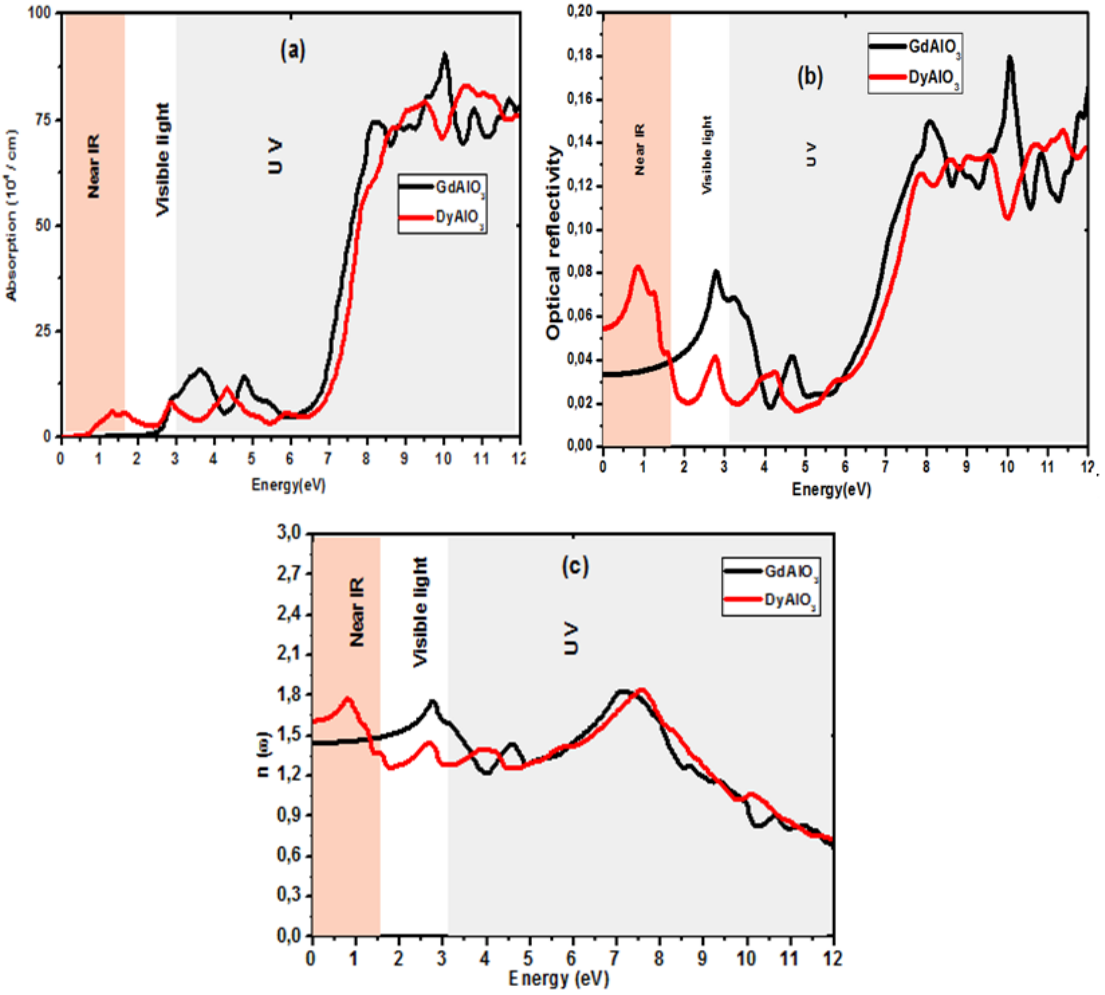


Figure 8. Absorption coefficient (a), reflectivity(b) and refraxion index (c) of $GdAlO_3$ and $DyAlO_3$

The absorption coefficient α(ω) (Figure 8.a) shows very intense absorption in the range 0.8-12 eV, the absorption of $GdAlO_3$ is zero In the infrared region, we observe very weak

absorption for the two cubic perovskites $GdAlO_3$ and $DyAlO_3$ due to the shift of electrons from the Dy -5s state to the O-2p state for the compound $DyAlO_3$ and from the Gd -5d state to the O-2p state for $GdAlO_3$. In the ultraviolet range, all compounds are considered good absorbers with different intensities. Maximum absorption is observed at around 10.31 eV and 10.75 eV for $GdAlO_3$ and $DyAlO_3$ perovskites respectively. It begins to increase sharply from 0.72 eV for $GdAlO_3$ and 2.54 eV for $DyAlO_3$, corresponding to the band gap value.

The refractive index Figure 8c) shows the trend in the $\varepsilon_1(\omega)$ values of the refractive index n(0) at low frequencies. The zero-frequency limit of the refractive index is 1.48 for $GdAlO_3$ and 1.63 for $DyAlO_3$, with a maximum value of 7.22 eV for $GdAlO_3$, and 7.76 eV for $DyAlO_3$. Consequently, we can define another very important parameter: the reflection coefficient k(ω), which characterizes the portion of the energy reflected at the solid interface. According to Figure 8.b, the zero-frequency limit of the reflectivity of $GdAlO_3$ is 0.034 and 0.053 for $DyAlO_3$. There are high reflection peaks at energies 10.25 and 11.37 eV corresponding to $GdAlO_3$ and $DyAlO_3$ respectively.

5. Conclusions

In the presented work, the calculations of structural and optoelectronic properties of cubic perovskites of type $XAlO_3$ (X = Gd, Dy) in the cubic phase were carried out using an ab -initio method known as the linearized augmented plane wave method with total potential FP-LAPW within the framework of the density functional (DFT) and using two approximations namely the generalized gradient approximation of Perdew-Burke-Ernzerhof (GGA-PBE) and the modified Becke-Johnson potential (mBJ) for the purpose of determining the exchange and correlation potential which are implemented in the Wien2k calculation code.

As a first step, we studied the equilibrium structural properties by determining the lattice parameters a0the compressibility modulus B and its derivative B' and the mesh volume V_0 using the GGA-PBE approximation. Our parameters and relaxed atomic positions are in good agreement with another theoretical study carried out with GGA-PBE.

In the second part, our calculations of electronic band structure and Density of states for the compound $GdAlO_3$ reveal a semi-conducting character with the presence of an energy gap: indirect at the L and xG points noting that the values of the energy gaps determined by the GGA approximation are low however the use of the mBJ approximation to improve the gap values considerably. and the compound $DyAlO_3$ behaves like a metal oxide.

The calculated of optical properties for both compounds, such as dielectric function,

refractive index, absorption coefficient and optical conductivity. They indicate that $GdAlO_3$ and $DyAlO_3$ perovskites could be useful for UV photocatalysis applications.

Finally, the results of our work seem very satisfactory, and we can vouch for the reliability and power of the FP-LAPW method. The results obtained are encouraging and have enabled us to predict certain characteristics of these materials. We therefore hope that our theoretical study will motivate researchers to study these properties experimentally.

References

[1] M. Sahnoun, M. Zbiri, C. Daul, R. Khenata, H. Baltache, M. Driz, *Materials Chemistry and Physics* **91**(1)(2005) 185

[2] R.L. Moreira, A. Dias, *J.Phys-Chem.Solids*. **8**(8)(2007)1617

[3] L.Q. Jiang, J.K. Guo, H.B. Liu, M. Zhu, X. Zhou, P. Wu, C.H. Li, *Journal of Physics and Chemistry of Solids* **67**(7) (2006)1531

[4] R. Ramesh, N.A. Spakiin, *Nature Mater* **6**(1) (2007)21-29

[5] J.F. Scott, *J.CondensMatter-Phys*. **18**(17)(2006)R361

[6] A. A. Bokov, Z.G. Ye, *J.Mater.Sci*. **41**(2006)31

[7] R.M. Ormerod, *Chem.Sov.Rev*. **104**(10)(2004)4845

[8] Y.H. Huang, R.I. Dass, Z.L. Xing, J.B. Goodenough, *Science* **312**(5771)(2006)254

[9] A. Gupta, B.W. Hussey, T.M,Shaw, *Mater.Res.Bull*. **31**(12)(1996)1463

[10] W. Eerenstein, N.D. Mathur, J.F. Scott, *Nature-London* **442**(7104)(2006)759

[11] A.S. Verma, A. Kumar, S.R. Bhardwaj, *Status Solidi. Phys*. B. **245**(8)(2008)1520

[12] D.M. Smyth, *Rev.Mater.Sci*, **15** (1)(1985)329

[13] A. Hossain , S. Roy and K. Sakthipandi, *Ceramics International*, 45 (4) (2019) 4152

[14] H. Fu, R.E. Cohen, *Nature A*, **403** (6767)(2000)281

[15] Y. Yamasaki, H. Sagayama, N. Abe, T. Arima, K. Sasai, M. Matsuura, K. Hirota, D. Okuyama,Y. Noda,Y. Tokura, *Phys.Rev.Lett.,* **101**(9)(2008)097204

[16] B. Ilschner, Ch. Janot, *PPUR presses polytechniques,* **19**(2001)118

[17] A. Waintal, *Solides State Communications*, **3**(1966)125

[18] R. Von Der. *Solides State Communications*, **31**(3)(1979)151

[19] B. Lorenz, Y.Q. Wang, Y.Y. Sun, C.W. Chu, *Phys.Rev.B*, **70**(21)(2004)212412

[20] S.C. Miller, W.F. Love, Tables of Irreducible Representations of Space Groups, (1967)

[21] K.S. Song, H. Xing-Cui, S-D. Kim, S-K. Kang, *Catal.Today,* **47**(1-4) (1999)155

[22] P. Durán, J. Tartaj, F. Capel, C. Moure, *J.Ceram.Soc.***24** (1) (2004). 2619

[23] M. Shelef, G. W. Graham, R. W. McCabe, *Catalytic Science Series*, **2**(2002)343

[24] H. Bali, B. Raveau, *Mat.Chem.Phys*. **8**(5)(1983)469

[25] G. Demazeau, *J. Développements Technologiques et Scientifiques*, **12**(9)(2009)933

[26] M. Ghedira, J. Marcus, J. Mercier, and C. Schlenker, *J. Chim. Sol.* **47** (1983) (113)

[27] S. Gariglio, J.M. Triscone, *Comptes Rendus Physique*, **12**(5-6)(2011)591

[28] R.Von Der, *Solides State Communications*, **31**(3)(1979)151

[29] P. Guillaume, *Comptes Rendus Chimie*, **12**(6-7)(2009)731

[30] Chun-lian Hu, *Solide State Communications*, **149**(7-8)(2009)334

[31] S. Nirpendra, J.R. Yul, *Journal of the Korean Physical Society*, **53** (2008) 806

[32] J.P. Monthéard, *European polymer journal*, **24**(12)(1988)1155

[33] C.Wu, F. Feng and Y. Xie, *Chemical Society Reviews,* **12** (2013)

[34] J.G. Mc Carty and H. Wise, *Catalysis Today*, **8**(2)(1990)231

[35] A. Kunioka, Y. Sakai, *Solid-State Electronics,* **8**(12)(1965)961

[36] N.Q. Minh, Ceramic fuel cells, *J.Am.Ceram.Soc*., **76**(3)(1993)563

[37] A. Reller, T. Williams, *Chemistry in Britain*, **25**(12)(1989)1227

[38] P. Blaha, K. Schwarz, G. K H Madsen, D. Kvasnicka, J. Luitz, R. Laskowsk, F.Tran, L. Marks, *WIEN2k: An Augmented Plane Wave Plus Local Orbitals Program for Calculating Crystal Properties*, **60**(1)(2001)

[39] T. Nakamura, *Chem.Lett*. (1974) 429.

[40] Z.Wu, R. E. Cohen, *Phys.Rev B*, **73**(23)(2006)235116

[41] F.D Murnaghan, *Proceedings of the National Academy of Sciences*, **30**(9)(1944)244

[42] B.O. Alsobhi, *Materials Chemistry and Physics* **301** (2023)127691

[43] T. Usman, J *Supercond Nov Magn*., **30**(2017)1389

[44] A. S. Verma, V. K. Jindal, *J.Alloys Comp*., **485**(1-2)(2009) 514

[45] R. Fouret, *Journal of Physics- Condensed Matter*, **9**(31)(1997)6579

[46] M. Maqbool, I. Ahmad, H. H. Richardson, M.E. Kordesch, *Appl.Phys.Lett*. **91**(19)(2007)

[47] B. Amin, I. Ahmad, M. Maqbool, J. Lightwave, *Technol*. **28**(2) (2010)223

[48] D. Anna, *Physical Review B***,** 54(3)(1996)1673

[49] D. Martin, G. Grüner, *Electrodynamics of solids* (2002)1269

[50] Kh. Dhahri, M. Bejar, E. Dhahni, M.J. Soares, M.F.P. Graca and M.A. Sousa, *Materials letters,*128(2014) 235

[51] Saji S. K., K. Raju and P. R. S. Wariar, *AIP Conf. Proc,*1728(1) (2016) 020602